Protein Structure

DOI: 10.1002/ange.201311203

Conformation and Topology of Diacylglycerol Kinase in *E.coli* Membranes Revealed by Solid-state NMR Spectroscopy**

*Yanke Chen, Zhengfeng Zhang, Xinqi Tang, Jianping Li, Clemens Glaubitz, and Jun Yang**

Abstract: *Solid-state NMR is a powerful tool for studying membrane proteins in a native-like lipid environment. 3D magic angle spinning (MAS) NMR was employed to characterize the structure of E.coli diacylglycerol kinase (DAGK) reconstituted into its native E.coli lipid membranes. The secondary structure and topology of DAGK revealed by solid-state NMR are different from those determined by solution-state NMR and X-ray crystallography. This study provides a good example for demonstrating the influence of membrane environments on the structure of membrane proteins.*

Structure determination of membrane proteins within the membrane environment with X-ray crystallography and solution-state NMR spectroscopy is a great challenge because of difficulties in generating quality crystals and the need to keep the correctly folded protein solubilized for an extended period of time. Consequently, various soluble membrane mimetics such as detergent micelles, isotropic bicelles, or nanodiscs have been developed and are applied to the structure determination of membrane proteins. Detergent micelles are the most commonly used membrane mimetics for X-ray crystallography and solution-state NMR. To date, the vast majority of membrane protein structures in the PDB have been determined in detergent environments. However, since the structures of membrane proteins are profoundly influenced by membrane–protein interactions,[1–6] structures determined in the membrane mimetic environments may differ from the corresponding structures in native membrane environments. Furthermore, the functional mechanism of many membrane proteins is intrinsically coupled to the lipid bilayer. Therefore, there is an increasing need to conduct structural studies in more native-like membrane environments to validate the 3D structures. However, it has historically been difficult to obtain sufficient structural data for membrane proteins under native-like membrane environments.

E.coli diacylglycerol kinase (DAGK) is an important enzyme, which phosphorylates diacylglycerol by using Mg^{II}-adenosine triphosphate (Mg-ATP; Figure 1 A).[7] Wild-type

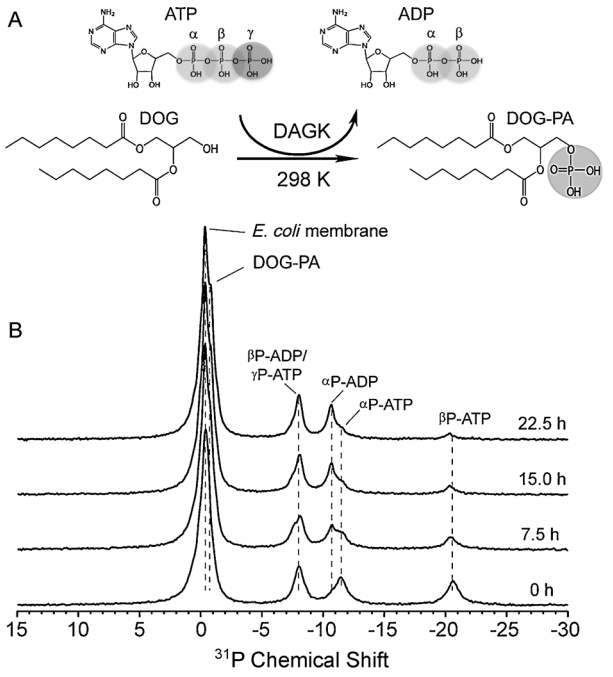

Figure 1. A) The enzymatic reaction of Mg-ATP and the lipid substrate 1,2-dioctanoylglycerol (DOG) catalyzed by DAGK. B) Under our experimental conditions at 23 wt% hydration, DAGK shows activity as monitored by ^{31}P MAS NMR. ATP is consumed and the DAG substrate DOG is phosphorylated. Upon increasing to full hydration, the activity is fully restored (Figure S4).

DAGK forms a 40 kDa homotrimer. The DAGK monomer is composed of an N-terminal amphipathic helix (AH) at the cytoplasmic side and three transmembrane (TM) helices. Two 3D structures have been reported for DAGK: one determined by solution-state NMR in dodecylphosphocholine (DPC) micelles and one by 3D crystallization in lipidic cubic phases (LCP).[8] Surprisingly, the two structures differ dramatically, a result that highlights the urgent need to analyze DAGK directly within lipid bilayers.

Magic angle spinning (MAS) solid-state NMR (ssNMR) is a powerful tool for studying the structures of membrane

[*] Y. Chen,[+] Dr. Z. Zhang,[+] X. Tang, J. Li, Prof. J. Yang
Key Laboratory of Magnetic Resonance in Biological Systems, State Key Laboratory of Magnetic Resonance and Atomic and Molecular Physics, Wuhan Center for Magnetic Resonance, Wuhan Institute of Physics and Mathematics, Chinese Academy of Sciences
Wuhan, 430071 (PR China)
E-mail: yangjun@wipm.ac.cn
Prof. C. Glaubitz
Institute for Biophysical Chemistry and Centre for Biomolecular Magnetic Resonance, Goethe University Frankfurt
Max-von-Laue Strasse 9, 60438 Frankfurt am Main (Germany)
[+] These authors contributed equally to this work.

[**] J.Y. acknowledges Humboldt Foundation fellowship. This work is supported by grants from the National Natural Science Foundation of China (21075133, 21173259) and DFG GL 3076-1. Plasmid pSD005 was provided by C.R. Sanders.
Supporting information for this article is available on the WWW under http://dx.doi.org/10.1002/anie.201311203.

proteins[9–11] directly within lipid bilayers[12–18] and even within whole cells.[19,20] In this study, 3D MAS NMR was employed to characterize the structure of DAGK reconstituted into its native *E.coli* lipid membranes. Approximately 80% of the amino acid residues of DAGK were assigned. Secondary structure and topology were identified by using these resonance assignments and H/D exchange experiments. Although the overall secondary structure and topology of DAGK revealed by ssNMR is consistent with the data from solution-state NMR and X-ray crystallography, notable differences exist, thus reflecting the interplay between the membrane environment and embedded proteins.

DAGK was expressed in *E.coli* cells, purified by affinity chromatography, and reconstituted into *E.coli* total lipid extract. To obtain high-quality liposome samples that yield high-resolution MAS NMR spectra, we screened a number of reconstitution variables, including lipid-to-protein ratios, pH values, and additives (Figure S1 in the Supporting Information). Additionally, we tested different hydration levels and found that 23 wt% hydration produces a good compromise between sensitivity and resolution (Figure S2). With 23 wt% hydration, ^{15}N and $^{13}C_{\alpha}$ signals in the 2D NCA spectra exhibiting average linewidths of approximately 85 and 150 Hz, respectively, can be obtained for U-^{13}C,^{15}N-DAGK samples. DAGK shows activity under the conditions used for solution-state NMR[21,22] and also when inserted into cubic lipid phases formed by monoolein, which was used for crystallization.[23] It is therefore important to also verify activity under the conditions used here. The approach used here, as described for DAGK by Glaubitz et al.,[24] allows the monitoring ATP turnover directly under MAS NMR conditions. At 23 wt% hydration, slow ATP turnover and DOG phosphorylation are observed, which is enhanced to its previously published values when increasing the hydration to 67 wt% (Figure 1B and Figure S4). These data, together with SDS-PAGE analysis showing DAGK as stable homotrimer, CD spectroscopy (Figure S5), and the fact that our well resolved 2D and 3D spectra show a single set of signals, demonstrate that the preparation procedure results in correctly folded, homogeneous, and functional samples.

With the careful optimization of both sample preparation and the NMR experiments, we were able to obtain assignments for approximately 80% of the residues when using a 600 MHz ssNMR spectrometer. The resonance assignments have been deposited in BMRB (accession number 19754). NMR experiments were performed at 277 K to ensure that the samples are in the gel phase without freezing the water, thereby maximizing the sensitivity and resolution.[25–28] To verify the chemical shift assignments, we also acquired 3D CONCA and NCOCX spectra for U-^{13}C,^{15}N and reversed-IL-labelled (natural abundance) DAGK samples (Figure 2 and Figure S6). All assigned residues are displayed in Figure 5B. Residue 1–13 of the N-terminus, 117–121 of the C-terminus, and 81–85 in the loop between TM helices 2 and 3 were not assigned because of their high mobility.

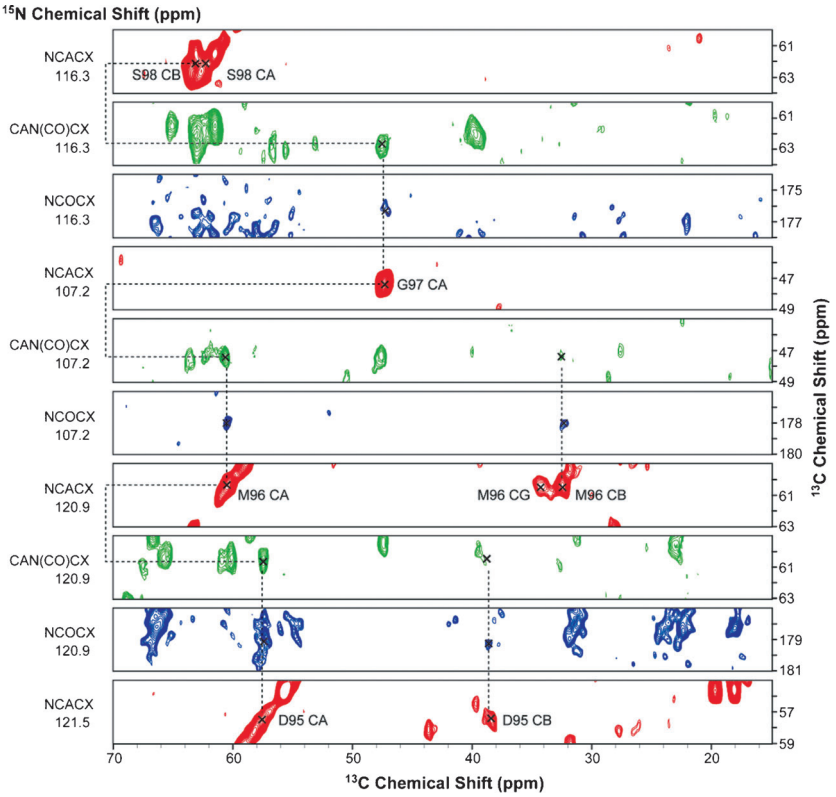

Figure 2. Representative sequential assignments of U-^{13}C,^{15}N-labeled DAGK based on a set of 3D NCACX, CAN(CO)CX, and NCOCX spectra with dipolar-assisted rotational resonance (DARR) mixing times of 10 ms, 20 ms, and 20 ms, respectively. The experiments were conducted on a 600 MHz NMR spectrometer at 277 K. The assignments of D95–S98 are indicated by dashed lines. The total measurement times were 114, 106, and 67 h for NCACX, CAN(CO)CX, and NCOCX, respectively.

The secondary structure of DAGK in *E.coli* membranes, as determined by a combination of TALOS+[29] and chemical shift index (CSI)[30,31] analysis, is compared in Figure 3 with the secondary structures obtained by solution-state NMR and X-ray crystallography. Although all three structures show a high α-helical content, there are notable differences. In contrast to the ssNMR data, the solution NMR structure shows two small distortions in Y16 within the AH helix and L70 of the TM2 helix. In addition, the loops between the AH and TM1 helix and between helices TM2 and TM3 are 4 and 7 residues longer, respectively, in DPC micelles compared to *E.coli* lipid bilayers. By contrast, the ssNMR-derived secondary structure agrees much better with the DAGK crystal structure. Only the loop between helices TM2 and TM3 is shifted from residues 81–85 in the ssNMR data to residues 87–91 (chain A), 86–91 (chain B), and 83–87 (chain C) of the X-ray structure[8] (Figure S9).

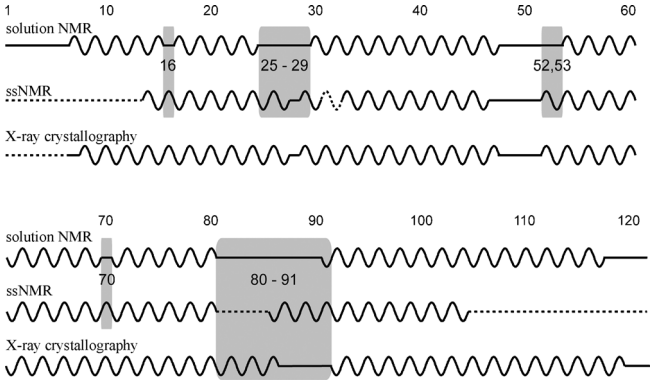

Figure 3. A comparison of DAGK secondary structures derived from solution NMR, solid-state NMR, and X-ray crystallography. The zigzag sections identify α-helical segments and the solid lines indicate residues that lack secondary structure. Residues that were not resolved by solid-state NMR or by X-ray crystallography are indicated by dash lines. The differences between the secondary structures determined by solution NMR and X-ray crystallography and that determined by ssNMR are highlighted in gray. The secondary structure of DAGK was determined from solid-state NMR by TALOS+[29] and chemical shift index (CSI)[30] based on chemical shifts (see Figures S7 and S8), while those determined by solution NMR (PDB 2KDC, wild type DAGK, chain A) and X-ray crystallography (PDB 3ZE5, Δ4-DAGK, chain A) are assigned by the DSSP software.[39] Δ4-DAGK, which was used in the ssNMR and X-ray studies, is a thermostabilized mutant with four amino acid residues changed relative to wild-type DAGK.

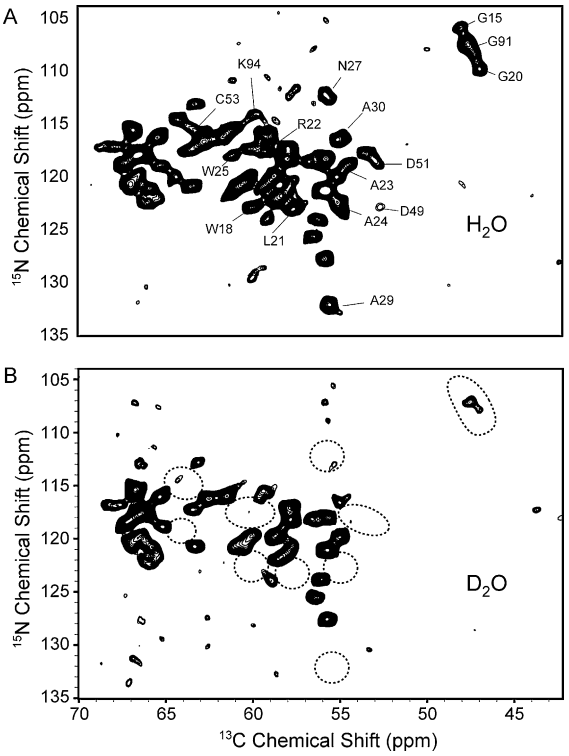

Figure 4. The water accessibility of U-^{13}C,^{15}N DAGK probed by 2D NCA spectra before (A) and after (B) H/D exchange. The peaks marked in (A) are signals from water accessible residues that disappear after H/D exchange (B; dashed circles). The experiments were conducted on a 600 MHz NMR spectrometer at 277 K.

To study the transmembrane topology of DAGK, we conducted H/D exchange[32] and corresponding MAS NMR experiments. It can be assumed that after three cycles of H/D exchange for 24 h at 310 K, the remaining NMR signals arise from non-exchangeable sites within the hydrophobic core of DAGK, while the residues with missing signals belong to extramembrane sites and flexible regions.[33] NCA spectra of U-^{13}C,^{15}N DAGK before and after H/D exchange are shown in Figure 4. Residue site-specific water accessibility of the protein was identified by comparison of 3D NCACX and NCOCX spectra of U-^{13}C,^{15}N-DAGK samples before and after H/D exchange (Figures S10 and S11). The topology of DAGK in *E.coli* membranes based on water accessibility is displayed in Figure 5 and compared to the topology derived from solution state-NMR in DPC micelles (based on ^{19}F NMR experiments[34]) and from 3D crystals as determined by the PPM server.[35] There are some important differences. The remaining NMR signals of some residues in the AH after H/D exchange means that these residues must be shielded from the solvent either by close contact with the cytoplasmic surface of the membrane and/or through close protein–protein contacts. By contrast, the solution-state NMR structure suggests that the AH points away from the protein core and the micelles and into the bulk solvent, a situation in which exchange would be expected. One reason could be the high micelle curvature (30–40 Å diameters[36]), which could interfere with the approximate diameter of the DAGK trimer (ca.100 Å).[22] Another difference is detected for TM2, which seems to be completely membrane embedded as judged from H/D exchange data, while more than 10 residues are solvent exposed on the cytoplasmatic side in DPC micelles, although this element has a similar length in both preparations. Furthermore, a number of residues in TM3 are water exposed in the DPC micelles but membrane embedded in lipid bilayers. The reasons for these differences could be the shorter chain length and the very high curvature of DPC micelles compared to almost planar lipid bilayers. This might also explain the differences between the X-ray structure and the ssNMR data, which show that fewer residues in TM2 and TM3 are solvent exposed in the lipid bilayer. The structure and topology of DAGK in 3D crystals might be affected by protein–protein crystal contacts and by the properties of the lipid cubic phases in which it was crystallized.

To date, the influence of the hydrophobic environment on the structure of membrane proteins has been extensively analyzed by comparing the structures of the single-TM protein influenza virus AM2 in three different solubilization environments.[1–3,37,38] Our study presents a comparison of the secondary structures of a multispan α-helical membrane protein in three different environments. Compared to the structure of DAGK in *E.coli* membranes, the solution NMR structure shows differences such as small distortions in AH and the TM2 helix, longer loops, and bending of the TM2 and TM3 helices, effects that are probably due to the high micelle curvature and smaller hydrophobic thickness. Although other factors such as mutations and different temperatures for solid-state and solution-state NMR experiments cannot be excluded as additional sources of structure perturbations,

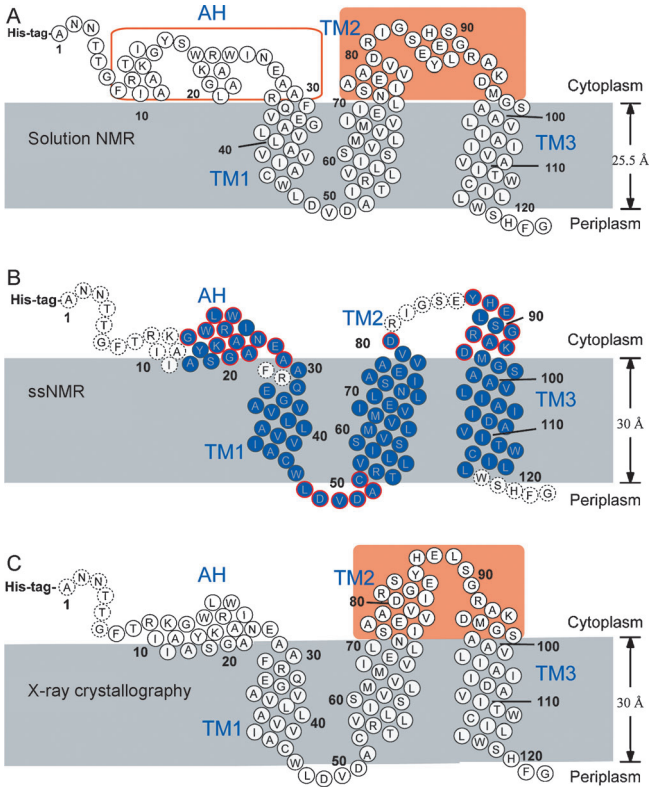

Figure 5. The topology of DAGK in three environments as determined by solution NMR[34](A), solid-state NMR (B), and X-ray crystallography (C). The hydrophobic regions are indicated by a gray background. The regions in the solution NMR and X-ray structures with different secondary structure from that of the ssNMR structure are highlighted in pink. The water-accessible residues probed by H/D exchange are marked with red circles in (B). The unassigned or unresolved residues are labeled with dash circles. The hydrophobic core of DAGK in *E.coli* membranes was identified based on the analysis of H/D exchange data. The hydrophobic boundaries of the protein were calculated by the PPM server[35] using X-ray (PBD 3ZE5) structures in (C).

the differences are likely due to the influence of the lipid/detergent environments. Clearly, the X-ray structure of DAGK shows more similarities to the solid-state NMR structure in terms of secondary structure and topology than the solution NMR structure. It should be noted that the variations in the secondary structures in the different environments all occur in catalytically critical regions such as the AH, cytoplasmic parts of the TM2 and TM3 helices, and the loop between the TM2 and TM3 helices. The conformational plasticity of these regions in the different environments is also likely a requirement for the enzymatic activity of DAGK.

In summary, we have presented the structural characterization of the three-TM protein DAGK in *E.coli* membranes by 3D MAS NMR spectroscopy. The secondary structure and topology of DAGK in *E. coli* membranes revealed by ssNMR are different from those indicated by solution NMR and X-ray structures, especially in the cytoplasmic surface regions. This work highlights the power of emerging ssNMR methods to probe the structure of multispan membrane proteins in membranes, and these solid-state NMR methods provide data highly compatible with X-ray crystallography data.

Received: December 25, 2013
Revised: February 5, 2014
Published online: April 2, 2014

Keywords: diacylglycerol kinase · membrane proteins · protein structures · solid-state NMR · structure elucidation

[1] D. T. Murray, N. Das, T. A. Cross, *Acc. Chem. Res.* **2013**, *46*, 2172–2181.
[2] T. A. Cross, M. Sharma, M. Yi, H. X. Zhou, *Trends Biochem. Sci.* **2011**, *36*, 117–125.
[3] S. Cady, T. Wang, M. Hong, *J. Am. Chem. Soc.* **2011**, *133*, 11572–11579.
[4] C. B. Kang, C. L. Tian, F. D. Sonnichsen, J. A. Smith, J. Meiler, A. L. George, C. G. Vanoye, H. J. Kim, C. R. Sanders, *Biochemistry* **2008**, *47*, 7999–8006.
[5] S. F. Poget, M. E. Girvin, *Biochim. Biophys. Acta Biomembr.* **2007**, *1768*, 3098–3106.
[6] K. Oxenoid, J. J. Chou, *Proc. Natl. Acad. Sci. USA* **2005**, *102*, 10870–10875.
[7] W. D. Van Horn, C. R. Sanders, *Annu. Rev. Biophys.* **2012**, *41*, 81–101.
[8] D. F. Li, J. A. Lyons, V. E. Pye, L. Vogeley, D. Aragao, C. P. Kenyon, S. T. A. Shah, C. Doherty, M. Aherne, M. Caffrey, *Nature* **2013**, *497*, 521–524.
[9] M. Hong, Y. Zhang, F. H. Hu, *Annu. Rev. Phys. Chem.* **2012**, *63*, 1–24.
[10] M. Renault, A. Cukkemane, M. Baldus, *Angew. Chem.* **2010**, *122*, 8524–8535; *Angew. Chem. Int. Ed.* **2010**, *49*, 8346–8357.
[11] A. McDermott, *Annu. Rev. Biophys.* **2009**, *38*, 385–403.
[12] M. Weingarth, A. Prokofyev, E. A. W. van der Cruijsen, D. Nand, A. M. J. J. Bonvin, O. Pongs, M. Baldus, *J. Am. Chem. Soc.* **2013**, *135*, 3983–3988.
[13] S. L. Wang, R. A. Munro, L. C. Shi, I. Kawamura, T. Okitsu, A. Wada, S. Y. Kim, K. H. Jung, L. S. Brown, V. Ladizhansky, *Nat. Methods* **2013**, *10*, 1007–1012.
[14] S. H. Park, B. B. Das, F. Casagrande, Y. Tian, H. J. Nothnagel, M. N. Chu, H. Kiefer, K. Maier, A. A. De Angelis, F. M. Marassi, S. J. Opella, *Nature* **2012**, *491*, 779–783.
[15] Y. M. Miao, H. J. Qin, R. Q. Fu, M. Sharma, T. V. Can, I. Hung, S. Luca, P. L. Gor'kov, W. W. Brey, T. A. Cross, *Angew. Chem.* **2012**, *124*, 8508–8511; *Angew. Chem. Int. Ed.* **2012**, *51*, 8383–8386.
[16] L. B. Andreas, M. T. Eddy, J. J. Chou, R. G. Griffin, *J. Am. Chem. Soc.* **2012**, *134*, 7215–7218.
[17] V. A. Higman, K. Varga, L. Aslimovska, P. J. Judge, L. J. Sperling, C. M. Rienstra, A. Watts, *Angew. Chem.* **2011**, *123*, 8583–8586; *Angew. Chem. Int. Ed.* **2011**, *50*, 8432–8435.
[18] S. D. Cady, K. Schmidt-Rohr, J. Wang, C. S. Soto, W. F. DeGrado, M. Hong, *Nature* **2010**, *463*, 689–692.
[19] M. Renault, R. Tommassen-van Boxtel, M. P. Bos, J. A. Post, J. Tommassen, M. Baldus, *Proc. Natl. Acad. Sci. USA* **2012**, *109*, 4863–4868.
[20] S. Reckel, J. J. Lopez, F. Lohr, C. Glaubitz, V. Dotsch, *ChemBioChem* **2012**, *13*, 534–537.
[21] J. Koehler, E. S. Sulistijo, M. Sakakura, F. J. Kim, C. D. Ellis, C. R. Sanders, *Biochemistry* **2010**, *49*, 7089–7099.
[22] W. D. Van Horn, H. J. Kim, C. D. Ellis, A. Hadziselimovic, E. S. Sulistijo, M. D. Karra, C. L. Tian, F. D. Sonnichsen, C. R. Sanders, *Science* **2009**, *324*, 1726–1729.
[23] D. F. Li, M. Caffrey, *Proc. Natl. Acad. Sci. USA* **2011**, *108*, 8639–8644.
[24] S. J. Ullrich, U. A. Hellmich, S. Ullrich, C. Glaubitz, *Nat. Chem. Biol.* **2011**, *7*, 263–270.

[25] W. B. Luo, S. D. Cady, M. Hong, *Biochemistry* **2009**, *48*, 6361 – 6368.
[26] B. B. Das, H. J. Nothnagel, G. J. Lu, W. S. Son, Y. Tian, F. M. Marassi, S. J. Opella, *J. Am. Chem. Soc.* **2012**, *134*, 2047 – 2056.
[27] K. D. Kloepper, D. H. Zhou, Y. Li, K. A. Winter, J. M. George, C. M. Rienstra, *J. Biomol. NMR* **2007**, *39*, 197 – 211.
[28] J. Yang, L. Aslimovska, C. Glaubitz, *J. Am. Chem. Soc.* **2011**, *133*, 4874 – 4881.
[29] Y. Shen, F. Delaglio, G. Cornilescu, A. Bax, *J. Biomol. NMR* **2009**, *44*, 213 – 223.
[30] S. Luca, D. V. Filippov, J. H. van Boom, H. Oschkinat, H. J. M. de Groot, M. Baldus, *J. Biomol. NMR* **2001**, *20*, 325 – 331.
[31] D. S. Wishart, B. D. Sykes, F. M. Richards, *Biochemistry* **1992**, *31*, 1647 – 1651.
[32] M. E. Ward, L. Shi, E. Lake, S. Krishnamurthy, H. Hutchins, L. S. Brown, V. Ladizhansky, *J. Am. Chem. Soc.* **2011**, *133*, 17434 – 17443.
[33] L. J. Catoire, M. Zoonens, C. van Heijenoort, F. Giusti, E. Guittet, J. L. Popot, *Eur. Biophys. J.* **2010**, *39*, 623 – 630.
[34] K. Oxenoid, F. D. Sonnichsen, C. R. Sanders, *Biochemistry* **2002**, *41*, 12876 – 12882.
[35] M. A. Lomize, I. D. Pogozheva, H. Joo, H. I. Mosberg, A. L. Lomize, *Nucleic Acids Res.* **2012**, *40*, D370 – D376.
[36] T. Lazaridis, B. Mallik, Y. Chen, *J. Phys. Chem. B* **2005**, *109*, 15098 – 15106.
[37] T. Wang, S. D. Cady, M. Hong, *Biophys. J.* **2012**, *102*, 787 – 794.
[38] F. H. Hu, W. B. Luo, S. D. Cady, M. Hong, *Biochim. Biophys. Acta Biomembr.* **2011**, *1808*, 415 – 423.
[39] W. Kabsch, C. Sander, *Biopolymers* **1983**, *22*, 2577 – 2637.

